



AMERICAN UNIVERSITY OF BEIRUT

TELEOPERATION OF UAV USING HAPTIC FEEDBACK

by  
ALI ABDEL KARIM KANSO

A thesis  
submitted in partial fulfillment of the requirements  
for the degree of Master of Engineering  
to the Department of Electrical and Computer Engineering  
of the Faculty of Engineering and Architecture  
at the American University of Beirut

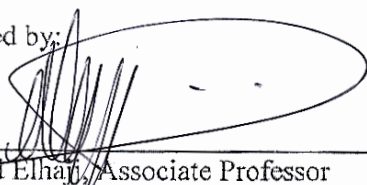
Beirut, Lebanon  
September 2015

AMERICAN UNIVERSITY OF BEIRUT

TELEOPERATION OF UAV USING HAPTIC FEEDBACK

by  
ALI ABDEL KARIM KANSO

Approved by:



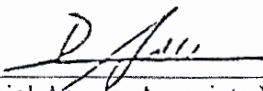
Dr. Imad Elhajj, Associate Professor  
Department of Electrical Engineering

Advisor



Dr. Ali Chehab, Professor  
Department of Electrical Engineering

Member of Committee



Dr. Daniel Asmar, Associate Professor  
Department of Mechanical Engineering

Member of Committee



Dr. Elie Shammas, Assistant Professor  
Department of Mechanical Engineering

Member of Committee

Date of thesis defense: September 28, 2015

# AMERICAN UNIVERSITY OF BEIRUT


## THESIS, DISSERTATION, PROJECT RELEASE FORM

Student Name: \_\_\_\_\_ Kanso \_\_\_\_\_ Ali \_\_\_\_\_ Abdel Karim \_\_\_\_\_  
Last First Middle

Master's Thesis       Master's Project       Doctoral Dissertation

I authorize the American University of Beirut to: (a) reproduce hard or electronic copies of my thesis; (b) include such copies in the archives and digital repositories of the University; and (c) make freely available such copies to third parties for research or educational purposes.

I authorize the American University of Beirut, **three years after the date of submitting my thesis** to: (a) reproduce hard or electronic copies of it; (b) include such copies in the archives and digital repositories of the University; and (c) make freely available such copies to third parties for research or educational purposes.



Signature

September 28, 2015

Date

## ACKNOWLEDGMENTS

Firstly, I want to express my sincere gratitude to my advisor Dr. Imad Elhajj for his guidance, support, patience, and understanding. I also would like to thank my committee members, Dr. Ali Chehab, Dr. Daniel Asmar, and Dr. Elie Shammass for their help and support on this project.

My sincere gratitude also goes to my family, especially my dad, and to my close friends Noel and Serge for their continuous support.

I also would like to thank Naim Bains for his efforts in creating the simulator environment. Also, I thank the members of the Vision and Robotics Lab at AUB for their patience. As well, I would like to thank Mr. Khaled Joujou, Mr. Salam Abyad, and Mr. Ali Kaafarani for their unconditional support during my master thesis.

I would like to thank everyone who participated in this research testing, without you this work would not be fruitful.

I would like to acknowledge the AUB University Research Board and the Lebanese National Council for Scientific Research for funding this project

# AN ABSTRACT OF THE THESIS OF

Ali Abdel Karim Kanso

for

Master of Engineering

Major: Control Systems

Title: Teleoperation of UAV Using Haptic Feedback

Teleoperation or operation at a distance refers to the remote control that occurs between a human operator and a slave machine. The teleoperation process extends the presence of the operator and his ability to perform certain tasks. In this thesis, we study the variables that affect the performance of operators while teleoperating unmanned aerial vehicles (UAVs). We propose a new approach to remotely control UAVs using haptic force feedback. The UAV is controlled using joystick's velocity commands, and the haptic feedback is a repelling force proportional to the UAV's velocity. Our proposed method that entails sensing the UAV velocity and commanding it using velocity based gestures proved to be an easier and more intuitive method for flying UAVs and accordingly, resulted in enhanced performance. Our method decreased the total flight time by 15.5%, shortened the flight path by 14.5 %, and reduced landing overshoot by 27.6%, compared to the mode using position based commands. Besides that, it reduced the subjective workload by 20.5%. Moreover, in this thesis we provide a thorough investigation of the different modes to teleoperate UAVs and we demonstrate how using the UAV velocity as force feedback can be more effective and intuitive. The added force did not increase the users' subjective workload index but it improved the objective results.

# TABLE OF CONTENTS

ACKNOWLEDGMENTS .....	v
ABSTRACT.....	vi
ILLUSTRATIONS .....	ix
TABLES .....	x
Chapter	
1. INTRODUCTION .....	1
2. PREVIOUS WORK.....	4
A. Types of Haptic Feedback .....	5
1. Haptic Feedback for Obstacle/Collision Avoidance.....	5
2. Haptic Feedback for Teleoperation of Multiple UAVs .....	6
3. Haptic Feedback for Intuitive Teleoperation .....	7
3. SYSTEM DESIGN.....	9
A. Joystick Control .....	9
B. UAV Feedback Mapping .....	11
C. Other Teleoperation Methods .....	12
4. SIMULATION SETUP AND RESULTS .....	14
A. Evaluating the Teleoperation Modes .....	15
B. Results .....	16
C. Further Investigation.....	20
5. EXPERIMENTAL SETUP .....	24
A. Experiment Setup and Design.....	24
1. Haptic Device Handling .....	25
2. RC Transmitter Handling .....	26

B. Modes of Teleoperation .....	27
1. Mode RC: Using the RC Device .....	29
2. Mode Vel_noF: Joystick – Velocity Commands Without Force Feedback .....	29
3. Mode Vel_F: Joystick – Velocity Commands with Force Feedback .....	31
4. Mode Pos_noF: Joystick – Position Commands Without Force ...	31
5. Mode Pos_F: Joystick – Position Commands with Force .....	32
C. The Experimental Procedure .....	32
<b>6. EXPERIMENTAL RESULTS .....</b>	<b>35</b>
A. Recruitment and Data Collection.....	35
B. Results .....	36
1. Objective Results .....	37
2. Subjective Results.....	40
<b>7. CONCLUSION AND FUTURE WORK .....</b>	<b>44</b>
<b>REFERENCES .....</b>	<b>46</b>
<b>APPENDIX A .....</b>	<b>48</b>
<b>APPENDIX B .....</b>	<b>49</b>



# ILLUSTRATIONS

Figure		Page
1	A quadrotor showing the chassis and the four rotors and propellers.....	2
2	Teleoperation system setup showing the master's coordinate frame orientation and the UAV's axes of rotation .....	3
3	UAV teleoperation diagram.....	10
4	Webots simulator environment.....	15
5	Objective Results of Experiment 1, showing the average and the std. dev. of the distance traveled and the time taken to finish each mode.....	17
6	Objective Results of Experiment 2, showing the average and the std. dev. of the distance traveled and the time taken to finish each mode.....	22
7	Testing room showing the quadrotor inside the safety net .....	25
8	Haptic device buttons.....	26
9	RC handling: thumb-prints on top of the control sticks and the tips of the index fingers on the side of the sticks.....	26
10	The RC controlling sticks and their operations .....	27
11	Step response to the fading function.....	30
12	Top view of the map .....	33

## TABLES

Table	Page
1 Teleoperation Modes .....	13
2 Targets location.....	15
3 P-values results of ANOVA test for mode 1 with the remaining modes.....	18
4 NASA TLX Workload Scores (percentage) .....	19
5 P-values results of ANOVA test of mode D with the remaining modes. ....	23
6 Objective results of the experiment on AscTec Pelican quadrotor.....	38
7 P-values for objective results - Time .....	39
8 P-values for objective results - Distance.....	39
9 P-values for objective results – Distance Overshoot .....	40
10 Subjective results of the experiment on AscTec Pelican quadrotor .....	41
11 P-values for objective results – NASA TLX .....	42

# CHAPTER I

## INTRODUCTION

Teleoperation or operation at a distance refers to the remote control that occurs between a human operator and a slave machine. The teleoperation process is used to extend the presence of the operator and his ability to perform the required tasks, while reducing mission costs and reducing threats on the operators. There are many forms of teleoperation and each has its own application and purposes. For example, teleoperation can be used to control ground vehicles [1], unmanned aerial vehicles [2], and underwater vehicles [3], or even to perform robot-assisted surgery [4]. In this thesis, we study the variables that affect the operators' performance in bilateral teleoperation of unmanned aerial vehicles (UAVs) with haptic feedback.

Unmanned aerial vehicles, UAVs, are a specific type of flying machines that do not require a human pilot onboard and can be remotely operated and controlled. In our research we are focusing mainly on the micro aerial vehicles and specifically the quadrotor (quadcopter) family; nonetheless, our findings can be extended to other types of aerial vehicles. The small size and agility of UAVs make such robotic platforms a great fit for wide range of applications in both military and civilian domains. For instance, UAVs have been used in military for surveillance and launching of military operations. Also, UAVs are used for search and rescue operations or in assessing harsh locations. UAVs are also used to inspect structures such as dams and bridges [5].



**Figure 1: A quadrotor showing the chassis and the four rotors and propellers**

A quadrotor UAV is composed of four rotors mounted on a rigid chassis as shown in Figure 1. Quadrotors can take off vertically, hover, and maneuver in restricted areas both indoors and outdoors. Because quadrotors are underactuated systems [6], a good understanding of their aerodynamics is necessary whether the machine is autonomously or human driven. Accordingly precise remote control of quadrotors is a challenging task because of the inherent loss of sensory perception while flying over a fast varying environment [7] and because of the need to control multiple parameters at once such as thrust, roll, pitch, and yaw.

UAV teleoperation is generally composed of three essential blocks: a flying robot (Slave), a ground station responsible for the bilateral communication (Channel), and an operator (Master), as shown in Figure 2. As such, there are three methods to remotely operate UAVs. In the first method, the UAV is operated in full autonomy; the UAV is moved from one place to another by setting the initial and final destinations. In this

mode, human operators are not responsible for the intermediated flying decisions between two consecutive waypoints. In the second method, the UAV is piloted by an operator who is monitoring and controlling its course from a fixed base on ground with a direct line of sight. Finally, the third method consists of piloting the UAV as if the operator was onboard (no direct line of sight); this mode requires sensory equipment such as cameras to explore the environment. In any of the three methods discussed above, situational awareness of the UAVs is very important to guaranty its safe and effective operation.

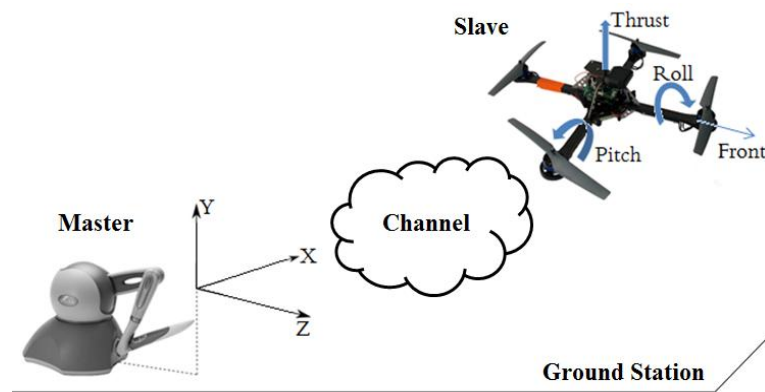


**Figure 2: Teleoperation system setup showing the master's coordinate frame orientation and the UAV's axes of rotation**

## CHAPTER II

### PREVIOUS WORK

In our research we are interested in the second method of controlling the UAV as discussed above. In this case, teleoperation is done manually by the operators who are in direct line of sight with the UAV and who are controlling it from a fixed ground station. In 2005 a study conducted for the American Department of Defense reported that 60.2% of UAV accidents were caused by or related to human factors [8]. Many may reason that the solution for this issue is by an increased automation of the flight process. However, it is difficult and challenging for a fully autonomous system to respond accurately and correctly to every arising event [7]. Therefore, human assessment is vital in particular cases such as military operations or rescue missions. Also, according to Hing and Oh [9], a UAV piloted in full autonomous mode may reduce the operators' level of situational awareness and their ability to react to emergencies.

Significant work has been conducted to increase the pilot's awareness and sensory perception using vision, haptic, and auditory feedback. Haptic feedback realized as force, motion, or vibration has been effectively used for flying UAVs. In [10], a study was conducted highlighting the importance of haptic over auditory feedback in improving the pilot's performance. Also in [11], the importance of this feedback was emphasized in reducing the number of collisions with degraded visual interface. In this thesis we propose a novel technique to teleoperate UAVs using a haptic device with force feedback. The control method aims at facilitating the flight process of UAVs by making it more natural and intuitive.

## **A. Types of Haptic Feedback**

Haptic feedback is widely used as an added sensory input to improve the system safety. The majority of work in the literature focuses on using the haptic feedback to sense the surrounding environment. For instance, the feedback may be related to the UAV position relative to an obstacle or to the distance to a destination point. However, few studies were done to relate the joystick commands and the haptic feedback to the internal properties of the UAV itself while aiming at making the flight process easier and more intuitive. Such feedback could be related to the “dynamics” of the UAV and the input commands should be intuitive.

### ***1. Haptic Feedback for Obstacle/Collision Avoidance***

Different types of force feedbacks have been investigated and the results show that the best way to avoid obstacles is by relating the force feedback to the velocity of the UAV while approaching the obstacle and the distance to impact [12], [13], [14].

Lam et al. [15] developed an artificial force field to map certain environmental constraints. Computer simulations were done to assess the efficiency of the force feedback in collision avoidance while teleoperating the UAV. They have concluded that haptic force feedback is a very helpful sensory input to the system.

Brandt et al. [14] used haptic force feedback for indoors UAV collision avoidance. They developed and compared three different algorithms for collision avoidance. The first algorithm is time-to-impact which is based on the quadrotor velocity and distance to the obstacle. The second is based on a dynamic parametric field; in this mode the force depends on which zone (safe, warning, transition, collision) the UAV is located in. In the third algorithm, the force is modeled as a virtual spring, where it varies linearly

with the distance to the obstacle. The test results of the time-to-impact and the dynamic parametric field show improvement over the virtual spring and no-force algorithms. This indicates that including the dynamics of the UAV in the calculation of the force feedback enhances the navigation process, thus reducing the number of collisions.

## ***2. Haptic Feedback for Teleoperation of Multiple UAVs***

The teleoperation of multiple robots is an active research topic involving both the autonomous swarming and human multi-robots interaction. Franchi et al. [16] used two haptic devices in order to control the bearing formation of multiple UAVs. The first device controls the UAVs motion and receives feedback of the UAVs velocity. The second device controls the bearing formation and receives forces related to the UAVs' expansion rate.

Moreover, Riedel et al. [17] presented a closed loop intercontinental teleoperation of multiple UAVs over the internet. Their work showed the system stability challenges because of the unreliable network and delays. They have used two types of feedback, the first one is the visual feedback in the form of video streams and the second one is the haptic feedback related to the UAVs' tracking performance. The force feedback is related to the difference between the set velocity and the actual one.

Lee et al. [18] proposed a semiautonomous teleoperation control architecture to pilot multiple UAVs with haptic feedback. They subdivided their teleoperation architecture into three control layers. At layer 1, they control each UAV individually to follow a desired trajectory. At layer 2, they control the location of UAVs with respect to each other and to the obstacles and that to avoid collisions. At layer 3, where



teleoperation takes place, the users can command some or all of the UAVs while receiving a haptic force feedback mapping the state of the UAVs.

### ***3. Haptic Feedback for Intuitive Teleoperation***

Ruesch et al. [19] propose a new technique based on kinetic scrolling in order to control the UAV motion without workspace constraints on the operator side. Accordingly, they make the gestures on the haptic devices similar to scrolling on touch displays. However, they map the joystick position in the master space to the UAV position in the slave space. Thus a more complex system is always needed to track the UAV in 3D space and a position controller must be implemented.

Omari et al. [20] presented an intuitive approach to teleoperate VTOL UAVs using haptic force feedback mapping the surrounding texture of the environment. Additionally, they teleoperate the UAV in position control mode and they implement an autonomous obstacle avoidance strategies. The limitation of this approach is that they are mapping the position of the haptic device end effector to the position of the UAV. Hence a position controller should be adopted to have an acceptable flight experience, which is difficult to accomplish using dead reckoning navigation. Also they used an add-on laser range scanner for obstacle detection and avoidance, thus losing the generality of their solution.

Xiaolei et al. [12] developed a new architecture to interconnect multiple haptic feedback devices. Their solution aims at solving the problems existing in position (joystick) to velocity (UAV) control in a natural and intuitive manner. As such they build a new haptic device in the shape of a trackball and interconnect it with another

haptic joystick. The new device renders impeding forces and the old device renders admitting force feedback.

To the best of our knowledge, the use of haptic devices in order to make the UAV teleoperation easier and intuitive is poorly addressed in the literature. The main focus is on sensing the surrounding environment instead of focusing on the UAV's internal parameters. Moreover, all commands used to drive UAVs using haptic devices are related to the joystick's end-effector change in position; there is no previous work done relating the joystick's velocity to the UAV motion and no comprehensive study comparing the different possible modes of operation. Our main contribution is to propose a new teleoperation system with intuitive and natural interface that allows users with no particular piloting skills to fly UAVs efficiently and safely.

## CHAPTER III

### SYSTEM DESIGN

In order to make the piloting process more natural and intuitive the haptic feedback is used to complement the visual one. As shown in Figure 3, we use the joystick's velocity to control the UAV with haptic force feedback proportional to the UAV's velocity in space. Our intuition behind this is to make the joystick commands and the haptic feedback similar in nature (velocity based) which should make the navigation of UAVs easier and more intuitive.

#### **A. Joystick Control**

The quadrotor motion is controlled in angle mode by sending the desired roll and pitch angles along with the thrust ( $\phi$ ,  $\theta$ ,  $T$ ); the yaw is kept constant at a zero rate. In this paper we limit our control parameters to three since the joystick we used has 3 degrees of freedom for haptic feedback.

The commands are directly proportional to the user's hand velocity. For example, if the user moves his/her hand faster in a certain direction, the UAV moves faster in that direction. As we shall demonstrate, this method proved to be more natural and more accurate than controlling the UAV using commands related to the joystick's change in position. Also, by using velocity commands we solve the workspace limitation of the haptic device, which exists when using the joystick's change in position as input to the system. Hence, the operator can move his/her hand slower or faster without the need for a larger workspace.

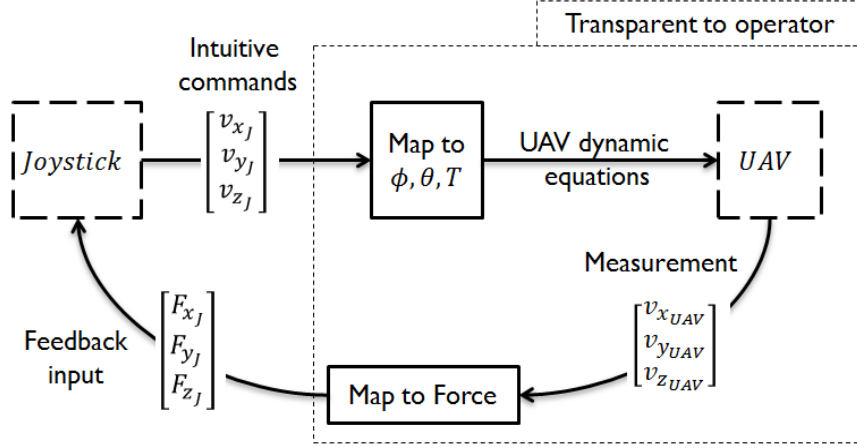


Figure 3: UAV teleoperation diagram

In order to enhance the teleoperation process and make it easier and more efficient, the nature of commands should be natural and intuitive from an operators' perspective. Hence, the UAV internal dynamic equations, the mapping of joystick commands, and the mapping to force feedback should be transparent to the operator. Since the yaw rate is equal to zero, the ground station coordinate frame and the UAV local frame have the same "orientation". Accordingly, the operators' sense of directions (left, right, forward, backward, up, and down) always matches that of the UAV. Hence, the joystick movements along the x-axis, y-axis, and z-axis are chosen to control the desired roll angle, desired thrust, and desired pitch angle of the UAV respectively as described in (1) to (3).

$$\text{Roll: } \varphi = k_1 v_{x_j} \quad (1)$$

$$\text{Pitch: } \theta = k_2 v_{z_j} \quad (2)$$

$$\text{Thrust: } T = k_3 v_{y_j} + T_{UAV} \quad (3)$$

where  $k_1$ ,  $k_2$ , and  $k_3$  are constants used to adjust the sensitivity of the commands.  $T_{UAV}$  is the current thrust value of the UAV and it is added to the thrust command in order to maintain the altitude when no commands are applied.  $v_{x_J}$ ,  $v_{y_J}$ , and  $v_{z_J}$  are the components of the joystick's velocity vector at each instance of time. Moreover, the roll and pitch angle values are limited between  $-\pi$  and  $\pi$  and the thrust is limited to positive values only.

Additionally, to prevent unwanted hand motion to be detected as commands, the users have to press a button located on the joystick's end effector whenever they want to command the UAV. This allows them to move their hand freely between consecutive commands. When the button is released, the desired roll and pitch angles are set to zero.

## B. UAV Feedback Mapping

The feedback applied to the joystick device acts as a repelling force resisting the user's hand motion. The force feedback is proportional to the opposite of the UAV velocity; hence preventing the operator from accelerating in a certain direction and avoiding high speed motions while enhancing his/her awareness of the UAV dynamics. Similar to the joystick commands mapping, the UAV sense of direction and its orientation match those of the joystick. Therefore, the UAV velocity in x, y, and z direction is mapped to a force feedback opposing its orientation. The mapping of UAV velocity to the force feedback vector components are shown in (4) to (6).

$$F_{x_J} = -k_4 v_{x_{UAV}} \quad (4)$$

$$F_{y_J} = -k_5 v_{y_{UAV}} \quad (5)$$

$$F_{z_J} = -k_6 v_{z_{UAV}} \quad (6)$$

where  $k_4$ ,  $k_5$ , and  $k_6$  are constants used to scale the intensity of the force feedback rendered by the joystick.  $v_{x_{UAV}}$ ,  $v_{y_{UAV}}$ , and  $v_{z_{UAV}}$  are the components of the UAV velocity at each instant of time. Also, the magnitude of applied force is limited to 3.3 N which is the maximum force rendered by the haptic device used in the experiment.

### C. Other Teleoperation Methods

In order to evaluate our proposed method which is based on velocity commands and UAV velocity feedback, we developed 5 other modes to compare against, and they are summarized in Table 1. The modes are divided into 2 categories based on the commanding method: joystick's velocity based commands and change in joystick's position commands. Moreover, we propose 3 types of force feedback for each commanding method: feedback based on the UAV velocity, feedback based on the distance from a target location, and no force feedback (used as benchmark).

Mapping of the joystick displacement into the desired UAV commands is done as shown in (7) to (9) below:

$$\varphi = k_7 \Delta P_{x_j} \quad (7)$$

$$\theta = k_8 \Delta P_{z_j} \quad (8)$$

$$T = k_9 \Delta P_{y_j} + mg \quad (9)$$

where  $\Delta P$  is the difference between the current position of the joystick's end effector and a fixed position determined by the operator when he/she initiated his/her current command using one of the joystick's buttons. In order to compensate for the loss in UAV elevation when hovering,  $mg$  is added to the thrust commands, where  $m$  is the

mass of the quadrotor and  $g$  is the gravitational constant. As such, the operators can maintain a fixed altitude when no commands are sent to the UAV.

Additionally, the distance of the UAV to each target point is mapped to force feedback as shown in (10) to (12) below:

$$F_{x_J} = -k_{10} (P_{x_{UAV}} - P_{x_{target}}) \quad (10)$$

$$F_{y_J} = -k_{11} (P_{y_{UAV}} - P_{y_{target}}) \quad (11)$$

$$F_{z_J} = -k_{12} (P_{z_{UAV}} - P_{z_{target}}) \quad (12)$$

Where  $P_{UAV}$  is the current position of the UAV and  $P_{target}$  is the location of the target point the pilot is trying to reach. As such, the force feedback is pointing towards the target. The  $k_i$  constants of all modes are chosen in a systematic way to make the most of the limited workspace area and the narrow force feedback margins of the haptic device. As such, we map the maximum and minimum reachable joystick's velocity and position to the limits of the roll, pitch angles and thrust. Similarly, the range of UAV velocities is mapped to the allowed range of force feedback rendered by the haptic device [-3.3; 3.3] Newton.

**Table 1: Teleoperation Modes**

<b>Mode</b>	<b>Command Type</b>	<b>Feedback Type</b>
1	Joystick velocity See (1) to (3)	UAV velocity, see (4) to (6)
2		UAV distance to target, see (10) to (12)
3		No force feedback
4	Joystick change in position See (7) to (9)	UAV velocity, see (4) to (6)
5		UAV distance to target, See (10) to (12)
6		No force feedback

## CHAPTER IV

### SIMULATION SETUP AND RESULTS

In order to assess the efficiency of the new proposed technique, a simulated environment was initially developed using Webots to implement the UAV dynamic equations and presented in [21]. The inputs to the open loop system are the roll, pitch, yaw and thrust. Measurement such as the UAV velocity and position can be taken directly from the simulator. The controller joystick used in the experiment is the Phantom Omni device from SensAble.

Furthermore, Using the Webots simulator, we have developed a flight course consisting of 4 waypoints placed at different locations as seen in Figure 4. The operator has to takeoff from a starting point on the ground and he/she should navigate the UAV through the 4 targets one after the other.

For illustration purposes we are showing the 4 target points location. However, the operator will only see one target at a time, and the next target will appear after passing through the current one. The targets' coordinates are shown in Table 2. The purpose of target 1 is to simulate a takeoff operation, where the operator commands the quadrotor through the first target after gaining some altitude. Besides, Target 2 and 3 are used to simulate a maneuvering technique by doing a sharp steering to the left and then to the right. The last target is located at longer distance, and it is used to test the operators' ability to reach the far target quickly. The shortest path (straight line) connecting the starting position and the 4 targets covers a simulated distance of 13.2 meters.



**Table 2: Targets location**

	X-Coordinate (m)	Y-Coordinate (m)	Z-Coordinate (m)
Starting Position	0	0	0
Target 1	1	2	0
Target 2	3	3	-1
Target 3	5	1	2
Target 4	8	4	1

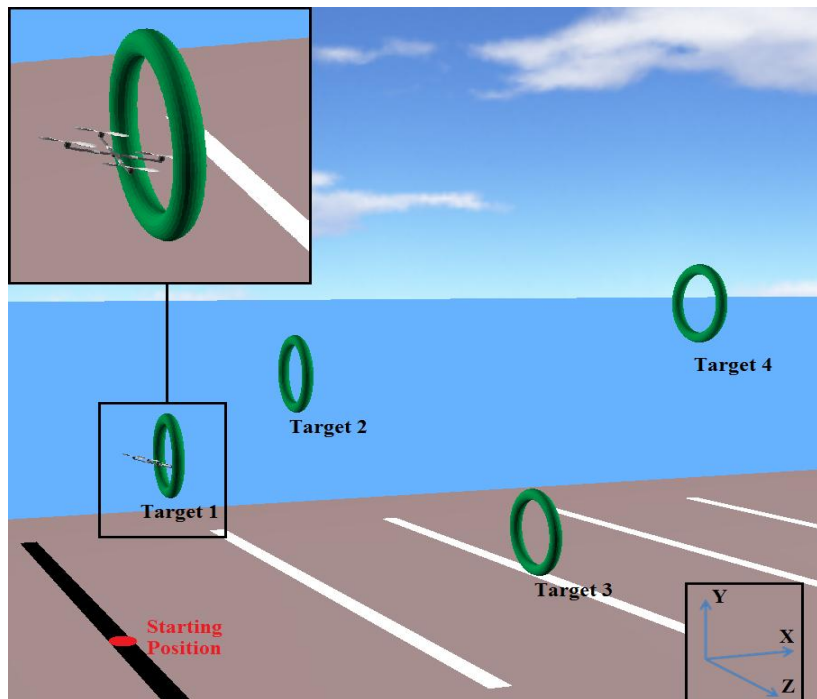


**Figure 4: Webots simulator environment**

### **A. Evaluating the Teleoperation Modes**

The efficiency of each mode is evaluated using objective and subjective measurements. The objective assessment is based on the time taken by the operator to finish the flight course and the cumulative distance traveled by the UAV. These two metrics combined will indicate how the operators performed per each mode. The

distance covered by the UAV is calculated by taking real-time measurements of the UAV position and accumulating the absolute difference in position readings. The distance metric is used to show whether the operators stayed on the planned path or they deviated from it. Moreover, the time metric is an indicator of the maneuvering ability of each mode by reaching the targets in shorter period of time. Hence a good flight mode will have a short flight time with minimum distance traveled.

Subjective measurements are taken using a survey based on the NASA Task Load Index (NASA-TLX). The NASA-TLX is a self-assessment score based survey widely used in human factors research (see appendix A). It measures the workload perceived by the participants on a scale from 0 to 100. The rating is based on a weighted average of 6 subscales dimensions: Mental Demands, Physical Demands, Temporal Demands, Own Performance, Effort and Frustration [22].

The experiment was conducted by four participants recruited from our lab and having no prior experience with UAV piloting and haptic feedback devices. It consists of 18 trials (each mode repeated 3 times), where the sequence of trials is random for each participant. This minimizes fatigue and training biasing the results. Additionally, the participants are subjected to a 30 minutes (5 minutes per mode) practice phase where they become familiar with the haptic device, the simulation environment, and the 6 piloting modes.

## **B. Results**

Figure 5 shows the average and standard deviation of the objective results (distance, time) for each mode of operation. The averaged data is calculated using the trials for all participants, and the standard deviation is shown using vertical lines.

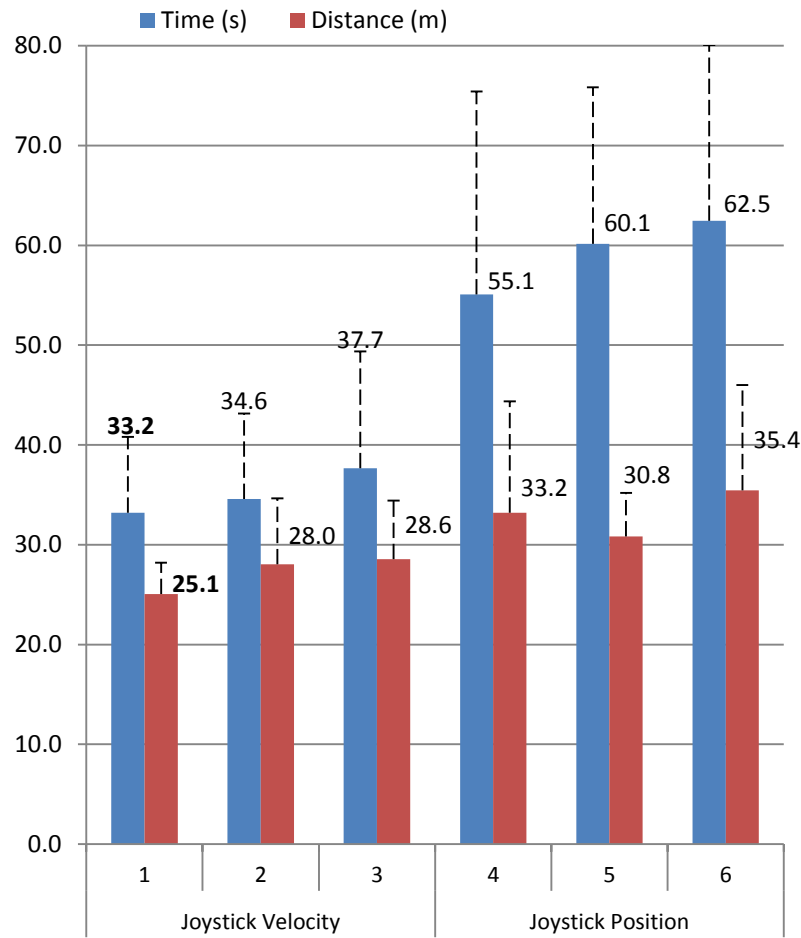


**Figure 5: Objective Results of Experiment 1, showing the average and the std. dev. of the distance traveled and the time taken to finish each mode.**

When using the joystick's velocity as commands (Mode, 1 2, and 3), operators are able to finish the flight course in 35.2 seconds, which is faster by 24.1 seconds comparing the modes using commands based on the change in position (Mode 4, 5, and 6). Hence the time per course is reduced by 41%. Similarly, the distance traveled is reduced by 18% from 33.2 meters for modes 4, 5, and 6 to 27.2 meters for modes 1, 2 and 3. Moreover, the standard deviation is smaller for the first three modes compared to the last three. This suggests that the modes using joystick velocity are more reliable and

consistent. Furthermore, combining velocity based commands with the UAV velocity based feedback (mode 1) shows the best performance in time and distance compared to the remaining modes. Accordingly, the operators performing in Mode 1 are not only faster at finishing the flight course but also they are closer to the shortest path. In order to analyze the significant differences between the mean of mode 1 and the other modes, the one-way Analysis of Variance (ANOVA) statistical test is conducted and the resulted p-values are shown in Table 3 below.

We have adopted a level  $\alpha=0.05$  in order to accept or reject the null hypothesis. Accordingly, using the velocity based commands as in Mode 1 shows a strong evidence against the null hypothesis (p-value<0.05 for modes 4, 5, and 6) and it has positive effect on the performance of the participants. There is no evidence against the null hypothesis when testing mode 1 against mode 2 and 3 and that's because these three modes have the same driving method using velocity commands.

**Table 3: P-values results of ANOVA test for mode 1 with the remaining modes.**

	Distance	Time
Mode 2	0.175619	0.684415
Mode 3	0.081969	0.280273
Mode 4	<b>0.023335</b>	<b>0.002075</b>
Mode 5	<b>0.001133</b>	<b>0.000022</b>
Mode 6	<b>0.003637</b>	<b>0.000027</b>

The qualitative results of the NASA-TLX survey results are shown in Table 4. Lower workload values indicate that the task at hand has low mental and physical demands, and its pace was not hurried or rushed. Also, a lower performance index indicates that the participants were satisfied with their results in accomplishing the task

goals. A low effort value indicates that the participants put a little work to accomplish their level of performance. Finally, a low frustration value indicates that participants were not discouraged or stressed during the task.

**Table 4: NASA TLX Workload Scores (percentage)**

Mode Subscale	Joystick Velocity			Joystick Position		
	1	2	3	4	5	6
Mental	<b>18</b>	30	22	53	47	48
Physical	<b>17</b>	27	20	58	55	50
Temporal	40	43	<b>38</b>	55	48	45
Performance	<b>13</b>	20	22	35	48	43
Effort	27	30	<b>23</b>	48	57	53
Frustration	<b>15</b>	22	<b>15</b>	25	40	48
Average	<b>21.7</b>	28.7	23.3	45.7	49.2	47.8
Total Average	24.6 ( $\sigma = 3.7$ )			47.6 ( $\sigma = 1.8$ )		
Std. Dev.	10.2	8.1	7.7	13.0	6.1	3.5
Total Std. Dev.	15.1			14.8		

The 6 subscales scores of the NASA TLX are equally weighted and their average value is presented in Table 4 along with their standard deviation, where the best score values are shown in bold font. When using joystick velocity commands, the score of each subscale of the 6 NASA-TLX survey measurements are better than those when using joystick change in position commands. Furthermore, the average of the total workload score while using joystick's velocity commands (Modes 1, 2, and 3) is equal to 24.6 ( $\sigma=3.7$ ). However, the average workload of modes using Joystick's change in position (Modes 4, 5, and 6) is equal to 47.6 ( $\sigma=1.8$ ). Moreover, the difference in the total standard deviation of the equally weighted subscales between the two commanding modes is negligible (less than 0.3). Hence, there is a 48.3% reduction in workload.

Consequently, our proposed method does not overload the operator and it is easier and more natural to use.

Moreover, combining velocity based commands with velocity based feedback (Mode 1) proves to be the most intuitive method to teleoperate UAVs. Using Mode 1, the mental demand score is the lowest compared to the other modes at a value of 18, meaning that the required task was not complex and it was fairly easy to complete. Besides, the physical demand is the lowest at a value of 17, implicating that the operators' hand movements involved in commanding the UAV was minimal within the joystick's small workspace. The temporal demand score at a value of 40 is slightly higher than that of Mode 3, which indicates that the pace of experiment was quicker and that is because the total time taken to finish the trials was much less as seen in Figure 5 (33.2 seconds for Mode 1 and 37.7 seconds for Mode 3). The overall performance score is the lowest at a value of 13, indicating that the operators were very satisfied with their results. But in order to achieve these successful results they have to put extra effort hence the score value of 27 on Effort scale. Frustration score is also the lowest in tie with Mode 3. This indicates that the operators where not stressed during the trials, and on the contrary they felt relaxed. Hence, velocity based force feedback does not add to the complexity of teleoperation and it combines coherently and efficiently with the velocity based commands.

### **C. Further Investigation**

After we verified the effectiveness of using joystick's velocity commands combined with the UAV velocity feedback, we conducted an in depth investigation concerning the nature of the force feedback mapping. The force feedback applied to the

joystick can be rendered in many forms. Regarding the direction of force vector, the feedback can be assisting (proportional to the UAV direction of motion) or a repelling one (opposing the UAV direction of motion). An assisting force feedback conveys to users the direction in which the UAV is currently moving, while a repelling force feedback restricts the users from commanding the UAV to move in the direction that it is already taking. Besides, the force can be continuously or discontinuously applied. In the continuous mode the user always senses the force feedback, whereas in the discontinuous mode user feels the feedback only when commanding the vehicle (while pressing the joystick's button). The experimental setup and design remained the same as experiment 1; the flight course consists as before of 4 waypoints placed at different locations as shown in Table 2. Each mode is repeated 3 times, in total of 15 trials and the sequence is randomly generated for each participant. Seven users participated in this experiment (same participants from the previous experiment plus three new) after finishing a practice phase of 25 minutes (5 minutes per mode). The different force feedback modes are: Mode A is continuous assisting, Mode B is continuous repelling, Mode C is Discontinuous assisting, Mode D is discontinuous repelling, and Mode E with no force feedback and it is treated as a benchmark.

As seen in Figure 6, the repelling type force feedback (Modes B and D) performs better than the assisting one (Modes A and C respectively). This result is attributed to the fact that repelling type forces resist the operators' abrupt commands. Additionally, repelling forces counteract the motion of the UAV which leads to better stability where the UAV will stay closer to the desired trajectory. Moreover, a repelling discontinuous type force feedback (Mode D) performs better than the remaining 4 modes. On average, the participants were able to complete the flight course in 20.7 seconds, and the UAV

covered a distance of 33.1 meters. In this mode, users are exposed to the feedback only when commanding the UAV; hence, their hand can move easily without any obstruction from the repelling force, allowing them to execute the next command more freely. Moreover, the standard deviation for Mode D is the lowest amongst all other modes, which implicates that this mode is the most consistent and most reliable.

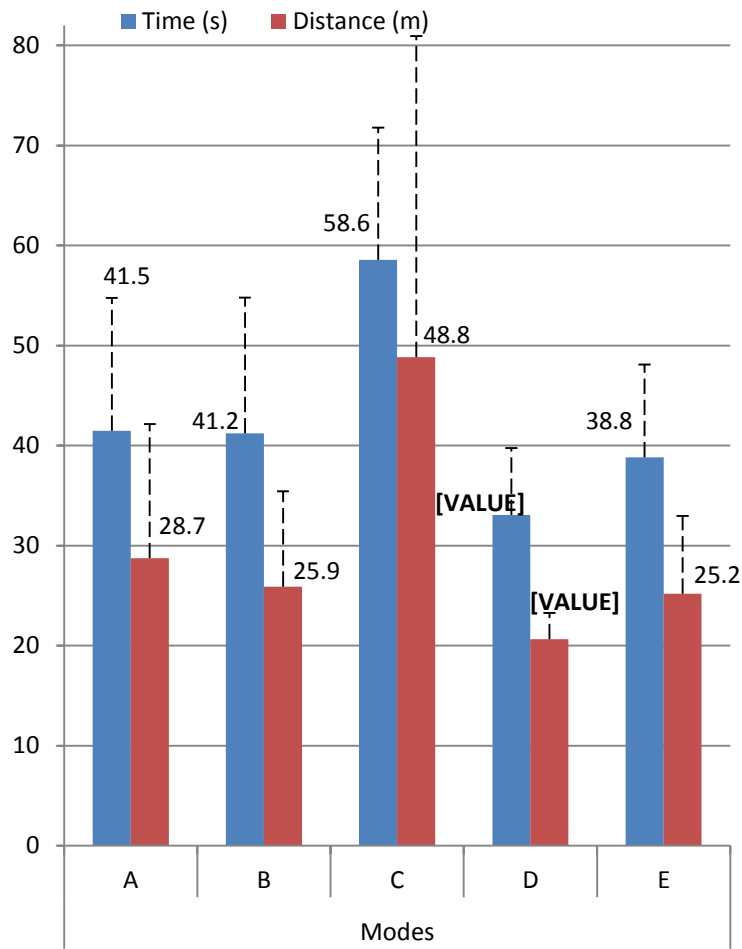


Figure 6: Objective Results of Experiment 2, showing the average and the std. dev. of the distance traveled and the time taken to finish each mode.

As earlier, we run the one-way ANOVA statistical test in order to analyze the significance of the differences between the mean of mode D and the other modes. The resulted p-values are shown in Table 5 below.



**Table 5: P-values results of ANOVA test of mode D with the remaining modes.**

	Distance	Time
Mode A	<b>0.034</b>	<b>0.037</b>
Mode B	0.055	<b>0.049</b>
Mode C	<b>0.0029</b>	<b>0.0000005</b>
Mode E	<b>0.045</b>	0.058

According to the p-values presented, using discontinuous repelling force feedback (mode D) shows strong evidence against the null hypothesis and it has positive effect on the performance of the participants. The p-value for the cumulative distance measurements in mode B and mode D is marginally higher than the adopted level  $\alpha=0.05$ . The same applies to the p-value of time traveled measurements for mode E and D; hence, the claim of null hypothesis rejection holds.

# CHAPTER V

## EXPERIMENTAL SETUP

This chapter describes the modes of teleoperations, experimental design and setup of testing our solution on a real quadrotor, the AscTec Pelican.

### A. Experiment Setup and Design

The second experiment is designed to validate the results we got using the simulator on a real quadrotor. This experiment employs a single SensAble PHANTOM OMNI® haptic device, a Futaba T7C remote controller (RC), and an AscTec Pelican quadrotor. While running the experiment, the participants were asked to use both the haptic device and the RC to fly the UAV. The participants were asked to sit in a place where they have a direct line of sight with the UAV while facing its back side.

The velocity of the UAV is measured using VICON system (because of the limitation of the hardware in use, where the velocity data of the UAV can only be transmitted when the GPS is enabled and running). The VICON system is a very precise measuring tool; it can measure up to mm precision. This precision can detect the slightest UAV vibrations thus making the force feedback more sensitive to noise. As such, we are sampling and averaging 5 samples at a time from the VICON system. Then we apply an Exponential Moving Average (EMA) filter to smoothen the data according to equation (15).

$$forces_{new} = forces_{current} \times \alpha + forces_{new} \times (1 - \alpha) \quad (13)$$

Where  $\alpha$  is a smoothing factor between [0; 1], and it was chosen to be equal to 0.2.

The testing took place in a laboratory room at AUB. For safety purposes, The quadrotor is put inside a net room as seen in Figure 7 below, where the walls and the ground is covered with a green construction safety net. The participants can see the quadrotor through the net without any obstruction.

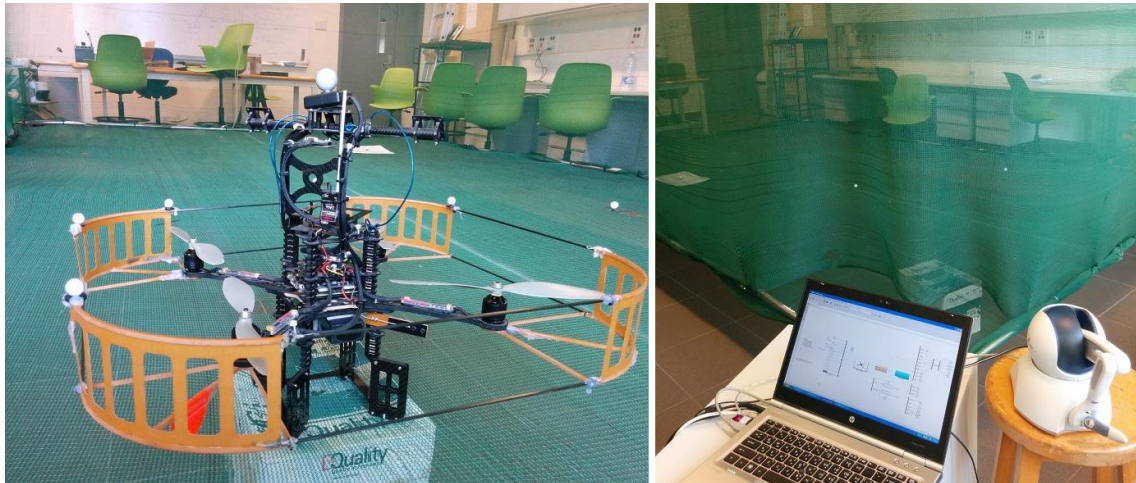


**Figure 7: Testing room showing the quadrotor inside the safety net**

### ***1. Haptic Device Handling***

The participants were required to hold the stylus of the PHANTOM Omni device as if they would hold a pen. Besides, there are two buttons located on the stylus pen as shown in Figure 8. The Participants should press button 1 (blue) to signal the start of each mode when they are ready (they will hear two consecutive beeps). Besides, they are required to use button 2 (white) each time they want to give a command to the vehicle during the experiment. Finally, they are required to press buttons 1 & 2 simultaneously once they complete each trial.

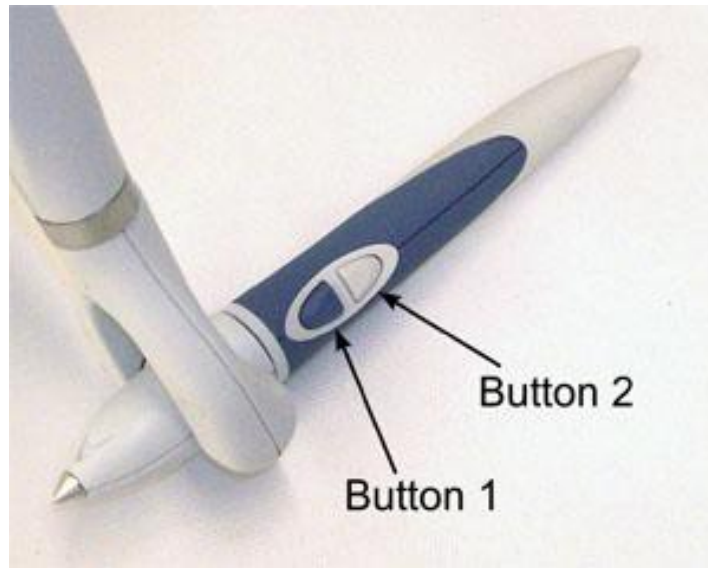


Figure 8: Haptic device buttons

## 2. *RC Transmitter Handling*

In modes where the participants use the RC for teleoperation, they were told to hold it firmly and put their fingers as shown in Figure 9 below. This technique reduces over-controlling and allows for precise commanding [23].

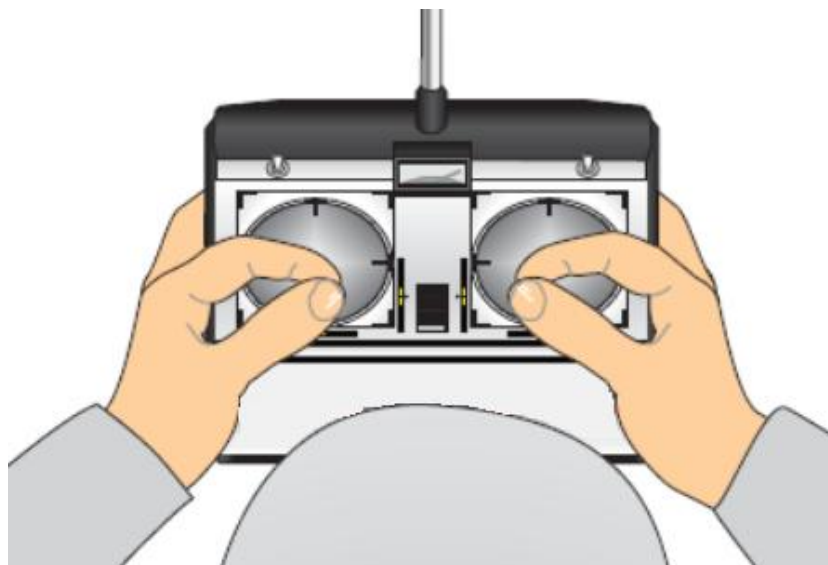


Figure 9: RC handling: thumb-prints on top of the control sticks and the tips of the index fingers on the side of the sticks

The participants were told how to interact with the RC sticks as seen in Figure 10 below; the left one for controlling the altitude and the right one for controlling the planar motion (left/right and forward/backward). Also, they were told not to move the yaw stick while driving the vehicle as this may cause the vehicle to rotate in place. Similar to the haptic devices, the participants should rotate the RC potentiometer clockwise to signal the start of the trial (they will hear two consecutive beeps) and counterclockwise once they complete each trial.

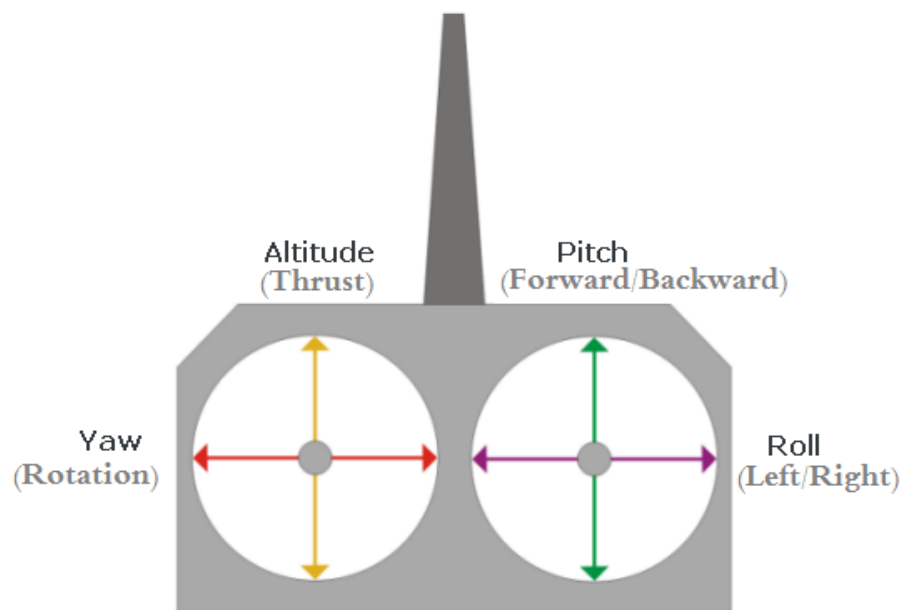


Figure 10: The RC controlling sticks and their operations

## B. Modes of Teleoperation

As we did in the simulator experiment, we tested our proposed method which is velocity based commands against the position based ones. Additionally, we introduced a new mode to compare against which is driving the UAV using the remote controller (RC). Moreover, we assume now that we are working in a GPS-denied environment

where no external sensors can point to the location of the Quadrotor while driving it. This is more realistic approach toward better testing the driving modes.

In addition to the mapping strategies discussed in Chapter III, we added extra features in order to cancel the effect of the UAV drifting when no input is applied. The drifting problem did not occur in the simulator because it was designed for an ideal scenario. In the case of a real quadrotor, there are multiple uncontrolled factors that can contribute to the drifting problems where even the on-board attitude controller cannot fix. Some of these factors include: misplacement of the battery that could shift the UAV center of mass, un-perfect calibration of UAV sensors (accelerometer, gyroscope, and magnetometer), chopped propellers, and wind turbulence from nearby objects.

The manufacturers are aware of such imperfection; where, they are solving this problem by adding trim switches on the RC that allow the pilots to bias the input they give to counter-effect the drift. Similarly, we are using a biased input in code to counter the effect of drift. The values that we uses are taken directly every time the experiment is run from the RC's trim switches and they are added to the commanding inputs.

This technique, using a fixed/constant bias, cannot eliminate the drift completely; as there are multiple parameters that contribute to the drift in the long run. As such, an alternative should be found to solve that issue taking into consideration that velocity based commands are zeroed when the users stop their hand movements.

The solution that we have adopted was inspired from the smart touchpad scrolling technique called coasting. Coasting or fading, is an option that allows users to scroll pages based on their last “velocity” input they apply on the touchpad. Similarly, we are recording the last velocity command the users used to command the UAV then we slowly fade it out to zero when the input is released (users stopped commanding).

### ***1. Mode RC: Using the RC Device***

In this mode the participants use a traditional 7-channels remote controller in order to fly the UAV. This method is considered as benchmark for other modes as it is the widely used method for driving UAVs in the market. The participants use both of their hands in order to give commands. Haptic feedback from the UAV is not applicable in this mode. Users rely on their visual feedback and on the haptic feedback they get from touching and moving the RC sticks.

### ***2. Mode Vel\_noF: Joystick – Velocity Commands Without Force Feedback***

In this mode, the participants use one haptic device to teleoperate the UAV. As we discussed in chapter III, the commands are based on the user's hand velocity which are then mapped to UAV commands (roll, pitch and thrust). In this particular mode no haptic feedback from the UAV is applied. The velocity of the haptic stylus pen controls the UAV motion. Moving the stylus pen faster or slower in a certain direction drives the UAV faster or slower respectively in the same direction. The upward/downward motion controls the altitude of the UAV. Moving in the upward direction increases the altitude of the vehicle and moving in the downward direction decreases its altitude.

Accordingly, the up/down motion are used to take off the ground, change altitude, and land. After taking off, users can use the left/right and front/back motion to move the UAV around the space toward a certain location.

The drift rejection techniques are only applied for roll and pitch inputs as seen in (14) and (15). The `fade_delay` and `fade_slope` are two parameters used to shape the fading function. The `fade_delay` determines how long the input will remain before it starts fading, and the `fade_slope` determines how fast the decay should be. Figure 11

shows the step response of the fading function with a fading scale equals to 5 and fading slope also equals to 5 (the values used during the experiment).

$$\text{Roll: } \varphi_{new} = \begin{cases} k_1 v_{xj} + \varphi_{bias}, & \text{command available} \\ \varphi_{old} \times \left(1 - \frac{1}{fade_{slope} + e^{-iteration + fade_{delay}}}\right), & \text{command released} \end{cases} \quad (14)$$

$$\text{pitch: } \theta_{new} = \begin{cases} k_2 v_{zj} + \theta_{bias}, & \text{command available} \\ \theta_{old} \times \left(1 - \frac{1}{fade_{slope} + e^{-iteration + fade_{delay}}}\right), & \text{command released} \end{cases} \quad (15)$$

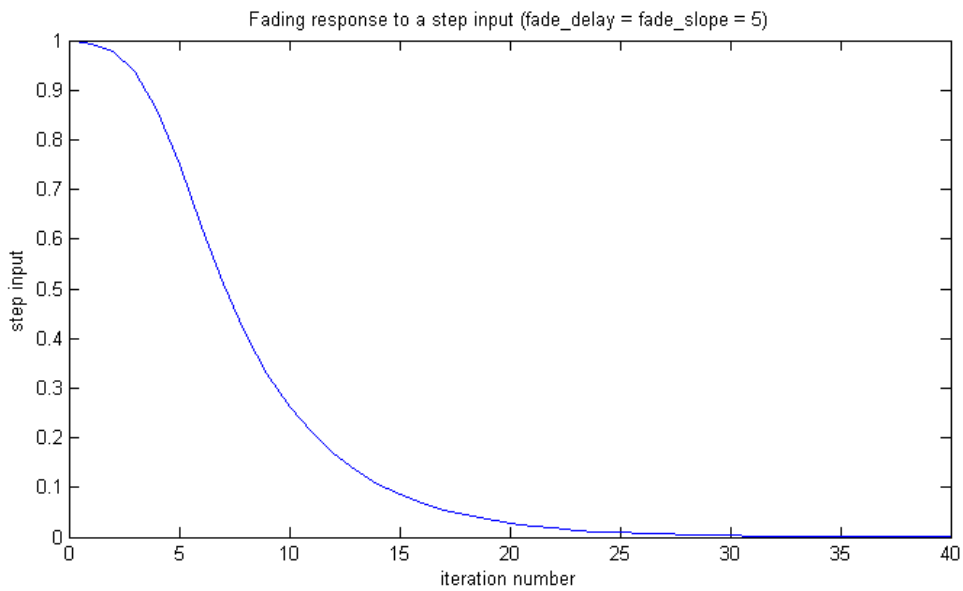


**Figure 11: Step response to the fading function**

In this mode there is no haptic feedback from the UAV. The participants rely on the visual feedback and the feeling they got from touching and moving the haptic stylus pen.



### **3. Mode *Vel\_F*: Joystick – Velocity Commands with Force Feedback**

Same commanding strategy as mode *Vel\_noF* presented above. However in this mode, the users sense a force feedback rendered by the haptic device. Similar to the haptic feedback presented in Chapter III, the force is inversely proportional to the UAV velocity. Meaning that they feel a repelling force if their hand motion direction is the same as the UAV one, and they feel an assisting force if their hand motion opposes the UAV one.

Additionally, the force feedback is applied only when the users are commanding the UAV and its velocity exceeding 0.1 m/s. This allows the users to move freely between commands and when the UAV is marginally stable.

### **4. Mode *Pos\_noF*: Joystick – Position Commands Without Force**

In this mode the participants use one haptic device to drive the vehicle. The UAV motion is controlled by the change in position of the stylus pen. The change in position is calculated as the difference between the current position of the stick and that when the user clicked the stylus pen. A bigger or smaller difference in position in a certain direction will drive the UAV faster or slower respectively in the same direction. The upward/downward motion controls the altitude of the UAV. Accordingly, the up/down motion are used to take off the ground, change altitude, and land. Also, the users can the left/right and front/back motions to move the UAV around toward a target location.

The drift rejection techniques used in the modes above (*Vel\_noF*, *Vel\_F*) are also adopted here as seen in (16) and (17). The biases, fading scales (delay, slope) are kept the same for consistency. The equations are show below.

$$\text{Roll: } \varphi_{new} = \begin{cases} k_8 \Delta P_{z_j} + \varphi_{bias}, & \text{command available} \\ \varphi_{old} \times \left(1 - \frac{1}{fade_{slope} + e^{-iteration + fade_{delay}}}\right), & \text{command released} \end{cases} \quad (16)$$

$$\text{pitch: } \theta_{new} = \begin{cases} k_8 \Delta P_{z_j} + \theta_{bias}, & \text{command available} \\ \theta_{old} \times \left(1 - \frac{1}{fade_{slope} + e^{-iteration + fade_{delay}}}\right), & \text{command released} \end{cases} \quad (17)$$

### 5. *Mode Pos\_F: Joystick – Position Commands with Force*

This mode has the same commanding strategy as mode Pos\_noF. However in this mode, the uses sense a force feedback rendered by the haptic device. The force is inversely proportional to the UAV velocity in space. Meaning that, the users feel a force against them if their hand motion is the same as the UAV and an assisting force if their hand motion opposes the UAV direction of motion.

The smoothing techniques of the haptic force feedback adopted in this mode are similar and consistent with the mode Vel\_F discussed above (averaging 5 samples and applying EMA filtering with  $\alpha = 0.2$ ).

### C. The Experimental Procedure

In order to eliminate the practice and fatigue effect, the five modes of teleoperation is randomized for each participant. Additionally, the sequence is repeated, in order, three times for a total of 15 trials per participant.

Accordingly, the experiment is divided into three phases, preceded by a 25 minutes practice phase (5 minutes for each mode). In each phase the five UAV teleoperation modes will be presented. The participants were required to fly the UAV along a designated course defined by a starting position, a checkpoint destination (UAV should pass in the 1.1 meter gap between tart1 and tar2 points), and a landing position

as seen in the top view of the map in Figure 12 below (the black dashed curve is an arbitrary flight path). At the end of each mode the participants were asked to fill a survey indicating their perceived workload (Mental Demand, Physical Demand, Temporal Demand, Performance, Effort, and Frustration) of the accomplished task.

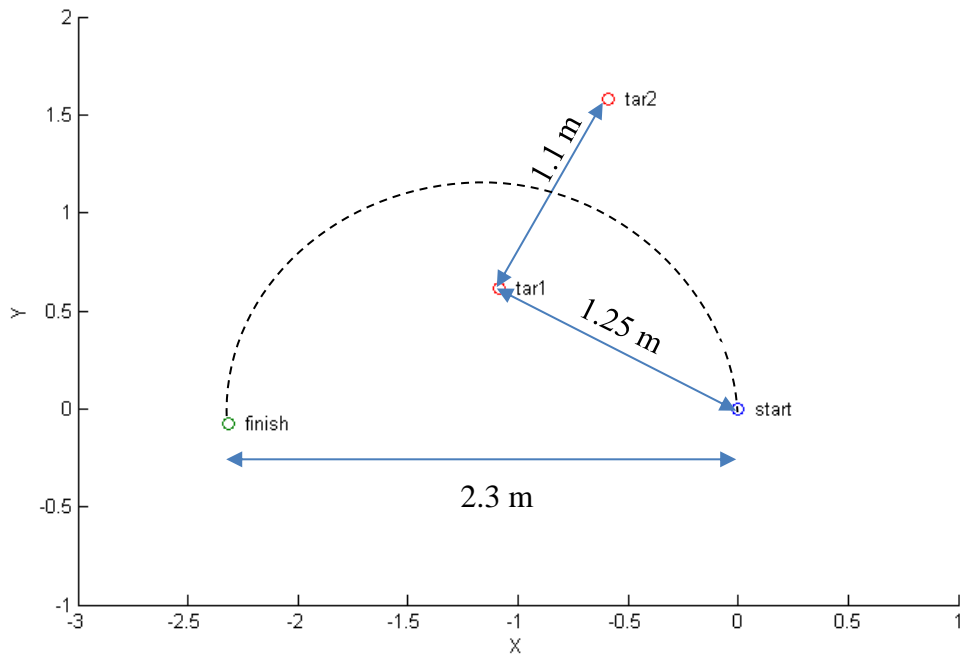


**Figure 12: Top view of the map**

The UAV is located initially at a starting position. Throughout the experiment the participants' orientation and the UAV's one will always be the same, where the UAV tail (marked by an orange patch) will always be facing the participants. Accordingly, the participants' sense of directions (left, right, forward, backward, up, and down) always matches that of the UAV.

Using the input device (RC or joystick), the participants were required to take off smoothly the UAV from the ground and drive it through a target location. The target location is indicated by two points on the ground where the participants were asked to keep the UAV between these two markers while driving over them. After that, the

participants were requested to land the UAV on a certain spot indicated by a special marker on the ground. Also, it was indicated that the time of the flight, and distance of the path taken are also a part of their subjective performance score.

# CHAPTER VI

## EXPERIMENTAL RESULTS

This chapter presents the statistical study of the subjects' performance participating in the experiment. It also shows how data (objective and subjective) are taken and stored. The obtained data is presented and analyzed. Finally, the significance of using velocity based command is assessed.

### **A. Recruitment and Data Collection**

Since the determination of the intuitiveness of our adopted method is subjective in nature, it is required to recruit as many participants as possible to validate the results. In total, 15 participants were able to complete the experiment successfully and the results that will discuss below are based on their data. All of the subjects were in the 18-35 years aging category, and all of them were right-handed. Additionally, there were 3 female and 12 male participants. There were 2 participants who were familiar with haptic devices, and in particular the Phantom Omni joystick. Among the participants, there were 5 persons who are considered video gamers, where they use gaming joysticks such as Xbox and PS controllers. This kind of experience can be a sign that they may have enhanced manual dexterity or improved cognitive and perceptual skills over other participants [24]. Additionally, none of the participants had a previous experience with flying aerial vehicles.

For the objective data collection, we are using VICON system to track the quadrotor's location in real-time while it moves inside the safety room. Additionally, we

are also storing the data we pulled from the quadrotor communication interface. All of the data is captured with a timestamp for later analysis; where each trial is stored in a data structure containing the user's Unique Identifier Code (UIC), mode name, trial number, and data tables. The data table is divided into columns containing the timestamp, quadrotor velocity coordinates, quadrotor position coordinates, feedback force applied coordinates, joystick velocity coordinate, joystick velocity position, joystick button status, quadrotor IMU Euler angles, quadrotor IMU rotation speed, quadrotor IMU acceleration, quadrotor IMU magnetometer.

For the subjective data collection, we are using a pen and paper based survey. The participants manually fill 15 pages of the NASA TLX survey corresponding to the order of their randomized sequence of trials. Moreover, the objective and the subjective data are matched together with the UIC number.

## **B. Results**

As before, the efficiency of each mode is evaluated using objective and subjective measurements. The objective analysis is based on 3 key parameters: time taken to finish the trial, cumulative distance traveled by the UAV till landing, overshooting from the chosen landing position. Besides that, there are counters for failed trials (major failure), hitting of the safety net (minor failure), and failing to pass through the target checkpoint. These quantitative metrics are indicators of the users' performance for each mode. They show objectively how each participant completed the task, whether they were able to perform the needed flight maneuvers more efficiently or not.

Furthermore, the modes are investigated subjectively using the NASA task load index survey. The rating is based on a weighted average of 6 subscales dimensions:

Mental Demands, Physical Demands, Temporal Demands, Performance, Effort and Frustration. The objective and subjective metrics combined will indicate how the operators performed in each mode.

### ***1. Objective Results***

The objective results of the experiment conducted on the AscTec Pelican quadrotor are shown in Table 6 (see appendix B). The values show the averaged data of the 45 trials performed by the 15 participants (3 trials each). The table also shows the standard deviation of averaged data along with the numbers of minor and major failures. “Failed once” metric counts the how many times the participants failed to complete the task of a certain mode but then succeeded after given a second chance. “Failed twice” counts how many times the participants failed to complete a trial out of the 3 available after given another second chance. After that their data for that trial is neglected, and they proceed with their test sequence.

As shown in Table 6, the mode Vel\_F which is velocity based commands with velocity based haptic feedback performed the best compared to the other modes. Besides, the results show that participants performed the worst in Pos\_noF and RC modes.

As for the time taken to finish each trial, participants using Vel\_F mode were able to finish the task in 11.3 seconds which shows a percentage reduction of -2.9 %, -16.9%, -15.5%, and -22.7 % compared to the modes Vel\_noF, Pos\_noF, Pos\_F, and RC respectively. Additionally the standard deviation is the lowest (1.81) among the other modes, which is an indicator of consistency.

**Table 6: Objective results of the experiment on AscTec Pelican quadrotor**

		Vel_noF	Vel_F	Pos_noF	Pos_F	RC
Time (s)	Mean	11.64	<b>11.30</b>	13.59	13.36	14.62
	Std. Dev.	2.37	<b>1.81</b>	3.42	2.17	4.60
	% change to Vel_F mode	-2.9%	-	-16.9%	-15.5%	<b>-22.7%</b>
Distance (m)	Mean	5.35	<b>5.04</b>	6.02	5.89	6.12
	Std. Dev.	0.80	<b>0.68</b>	1.37	0.85	1.51
	% change to Vel_F mode	-5.8%	-	-16.2%	-14.5%	<b>-17.5%</b>
OS (m)	Mean	0.40	<b>0.31</b>	0.64	0.44	0.44
	Std. Dev.	0.28	<b>0.18</b>	0.38	0.26	0.28
	% change to Vel_F mode	-20.5%	-	<b>-50.9%</b>	-27.6%	-28.2%
Not passing through checkpoint		<b>0</b>	<b>0</b>	<b>0</b>	<b>0</b>	2
Hitting net		<b>0</b>	<b>0</b>	4	2	3
Failed once		<b>0</b>	3	8	9	7
Failed twice		<b>0</b>	<b>0</b>	1	<b>0</b>	1

Moreover, the ANOVA test is also performed to validate the statistical significance of our findings. The P-values (one-tailed) between all modes are shown in Table 7 below. As before, we have adopted a level  $\alpha=0.05$  in order to accept or reject the null hypothesis. Hence, the P-values of Vel\_F mode shows a strong evidence against the null hypothesis ( $p\text{-value}<0.05$  for modes Pos\_noF, Pos\_F, and RC) and it has positive effect on the performance of the participants. There is no evidence against the null hypothesis when testing mode Vel\_noF and that's because this mode has the same driving method using velocity based commands.



**Table 7: P-values for objective results - Time**

	Vel_F	Pos_noF	Pos_F	RC
Vel_noF	0.46	0.00095	0.00024	0.000078
Vel_F	-	0.000054	0.0000018	0.000008
Pos_noF	-	-	0.63	0.18
Pos_F	-	-	-	0.061

Similarly, participants using Vel\_F mode completed the trials while traveling an average of 5.04 meters with the smallest standard deviation of 0.68. This mode showed a percentage improvement of -5.8%, -16.2%, -14.5 % and -17.5% compared to the modes Vel\_noF, Pos\_noF, Pos\_F, and RC, respectively. The P-values of ANOVA tests are shown in Table 8 below. The P-values for Vel\_F mode show a strong evidence against the null hypothesis ( $p\text{-value} < 0.05$  for modes Pos\_noF, Pos\_F, and RC). There is no evidence against the null hypothesis when testing mode Vel\_noF.

**Table 8: P-values for objective results - Distance**

	Vel_F	Pos_noF	Pos_F	RC
Vel_noF	0.097	0.0015	0.0019	0.0037
Vel_F	-	0.000018	0.000002	0.000072
Pos_noF	-	-	0.34	0.91
Pos_F	-	-	-	0.43

Regarding the landing location, participants using Vel\_F mode were able to land the UAV 0.31 meters nearby the landing mark (with 0.18 meters as standard deviation).. This mode showed a percentage improvement of -20.5%, -50.9%, -27.6%, and -28.2% compared to the modes Vel\_noF, Pos\_noF, Pos\_F, and RC, respectively. The P-values of ANOVA tests are shown in Table 8 below. The P-values for Vel\_F mode show a

strong evidence against the null hypothesis ( $p$ -value $<0.05$  for modes Pos\_noF, Pos\_F, and RC). There is no evidence against the null hypothesis when testing mode Vel\_noF.

**Table 9: P-values for objective results – Distance Overshoot**

	Vel_F	Pos_noF	Pos_F	RC
Vel_noF	0.25	0.0004	0.5	0.29
Vel_F	-	0.0000018	0.043	0.018
Pos_noF	-	-	0.002	0.0089
Pos_F	-	-	-	0.66

Lastly, the number of minor and major failures are less in modes adopting velocity based commands (Vel\_F and Vel\_noF) where only 3 failures are recorded and the participant were able to complete the trial when repeated. Additionally, we can notice that the participants in velocity based commands did not hit the safety net at all. On the other hand, the major and minor failure counts increases drastically for modes using RC and position based commands. It is noted that only in RC mode, there were 2 incidents recorded where participants were unable to recover from a failure after given a second chance. Besides, there was a total of 9 times where participants failed to complete the task from the first time with Pos\_F mode being used and 8 times when Pos\_noF is being used. Hitting the net without crashing is also recorded for Pos\_noF (4 times), Pos\_F (2 times), and RC modes (3 times).

## **2. Subjective Results**

Table 10 shows the averaged subjective data, where the 6 subscales of the NASA TLX are equally weighted. Also, it shows the individual averaging for each one of the 6 subscales (along with standard deviation and % change).

**Table 10: Subjective results of the experiment on AscTec Pelican quadrotor**

		Vel_noF	Vel_F	Pos_noF	Pos_F	RC
6 subscales equally weighted	Mean	27.09%	<b>26.44%</b>	37.05%	33.28%	35.78%
	Std. Dev.	16.90%	<b>16.73%</b>	20.85%	17.96%	21.75%
	% change to Vel_F mode	-2.4%	NA	<b>-28.6%</b>	-20.5%	-26.1%
Mental Demand	Mean	27.44%	<b>27.27%</b>	35.91%	33.33%	37.56%
	Std. Dev.	<b>13.89%</b>	15.28%	18.07%	17.51%	21.87%
	% change to Vel_F mode	-0.6%	NA	-24.1%	-18.2%	<b>-27.4%</b>
Physical Demand	Mean	25.78%	<b>24.77%</b>	35.00%	31.67%	29.07%
	Std. Dev.	15.60%	<b>15.04%</b>	19.51%	15.95%	22.45%
	% change to Vel_F mode	-3.9%	NA	<b>-29.2%</b>	-21.8%	-14.8%
Temporal Demand	Mean	<b>26.22%</b>	26.48%	33.75%	31.67%	36.40%
	Std. Dev.	16.67%	<b>16.50%</b>	19.66%	17.16%	21.92%
	% change to Vel_F mode	1.0%	NA	-21.5%	-16.4%	<b>-27.3%</b>
Performance	Mean	27.89%	<b>27.05%</b>	44.66%	36.22%	40.23%
	Std. Dev.	17.56%	<b>16.28%</b>	23.07%	18.74%	19.14%
	% change to Vel_F mode	-3.0%	NA	<b>-39.4%</b>	-25.3%	-32.8%
Effort	Mean	33.78%	<b>32.73%</b>	41.25%	38.78%	37.21%
	Std. Dev.	20.03%	19.98%	19.49%	<b>17.42%</b>	21.33%
	% change to Vel_F mode	-3.1%	NA	<b>-20.7%</b>	-15.6%	-12.0%
Frustration	Mean	21.44%	<b>20.37%</b>	31.59%	27.98%	32.63%
	Std. Dev.	<b>14.93%</b>	14.98%	21.56%	18.48%	21.51%
	% change to Vel_F mode	-5.0%	NA	-35.5%	-27.2%	<b>-37.6%</b>

As seen in Table 10, the load index is always lower for modes adopting velocity based commands (Vel\_F and Vel\_noF). On average, the velocity commanding mode

with force feedback shows the lowest load index (26.44%) which is slightly better than the mode without force feedback (27.09%). Our method is able to decrease the workload by 2.4%, 28.6%, 20.5% and 26.1 % compared to modes Vel\_noF, Pos\_noF, Pos\_F, and RC, respectively. Moreover, the percentage differences between Vel\_F and Vel\_noF modes for the 6 different subscales are negligible, thus we can conclude that the added force feedback was improving the participants' performance without obstructing their movement or increasing their workload.

The P-values of ANOVA test is shown in Table 11. The P-values for Vel\_F mode show a strong evidence against the null hypothesis (p-value<0.05 for modes Pos\_noF, Pos\_F, and RC). There is no evidence against the null hypothesis when testing mode Vel\_noF.

**Table 11: P-values for objective results – NASA TLX**

	Vel_F	Pos_noF	Pos_F	RC
Vel_noF	0.66	2.61E-09	0.000045	4.12E-07
Vel_F	-	2.85E-10	0.0000071	6.24E-08
Pos_noF	-	-	0.025	0.49
Pos_F	-	-	-	0.15

If we analyze each subscale of the NASA TLX independently, we can see that Vel\_F and Vel\_noF modes share the same mental demand (27.27% and 27.44%), same physical demand (24.77% and 25.78%), same temporal demand (26.48% and 26.22%), same performance (27.05% and 27.89%), same effort (32.73% and 33.78%), and same frustration (20.37% and 21.44%). Hence, the adopted force feedback did not bias the participants' workload. Consequently, the UAV velocity mapped to force feedback was rendered naturally and it conforms homogeneously to the velocity command input.

On the other hand, the subjective workload of the remaining modes are improved considerably. The RC mode has the highest mental demand (37.56%), temporal demand (36.40%), and frustration (32.63%) and it was improved by 27.4%, 27.3%, and 37.6%, respectively. The Pos\_noF mode has the worst perceived performance (44.66%), highest physical demand (35.00%), and effort (41.25%). These workload indexes are improved by 39.4%, 29.2%, and 20.7%, respectively.

## CHAPTER VII

### CONCLUSION AND FUTURE WORK

This thesis first highlighted the background of teleoperation systems with haptic feedback. We showed the various challenges encountered while driving the vehicle using traditional teleoperation methods. We discussed the need for a new system that could be more intuitive and natural so users can use it to improve their UAV driving performance.

In this thesis, we presented a new intuitive technique for UAV teleoperation using joystick's velocity commands and discontinuous repelling force feedback. Sensing the UAV velocity and commanding it using velocity based gestures proved to be easier and more natural for flying UAVs. Based on extensive experimentation it was demonstrated that our method is qualitatively and quantitatively superior compared to other modes of teleoperation. The experimentation was firstly done using a flight simulator environment where multiple users tested the proposed method and validated our proposed claim. Furthermore, in order to have a full validation of our mode, we tested and compared it on a real quadrotor. The new testing included the traditional teleoperation device being the RC, along with the previously proposed methods.

As future work, a new method could make benefit from using multiple haptic devices in order to increase the system inputs (thus benefiting from input redundancy) and making the flight process more user friendly by adopting gesture based commands. As a consequence of introducing more degrees of freedom, the user would be able to apply yaw input to the UAV, which was not possible in currently presented method.

As a future work also, the constants needed for mapping the hands gestures to the teleoperation of the UAV can be controlled adaptively in order to ensure the best possible performance. This adaptation of parameters is going to reduce the work effort, reduce the roughness in input commands and regulate the fluctuation of input commands.

## REFERENCES

- [1] N. Murakami, A. Ito, JD Will, et. al., "Development of a teleoperation system for agricultural vehicles," in *Electrical & Computer Engineering, Valparaiso University, USA*, 2008.
- [2] A. Birk, B. Wiggerich, H. Bülow, et. al., "Safety, Security, and Rescue Missions with an Unmanned Aerial Vehicle (UAV)," in *Journal of Intelligent & Robotic Systems*, 2011.
- [3] G. Griffiths, *Technology and Applications of Autonomous Underwater Vehicles*, London New York: Taylor & Francis, 2003.
- [4] A. Okamura, *Methods for haptic feedback in teleoperated robot-assisted surgery*, The Industrial Robot, 2004.
- [5] R. Murphy, E. Steimle, and M. Hall, et al., "Robot-assisted bridge inspection after Hurricane Ike," in *Safety, Security & Rescue Robotics (SSRR)*, 2009.
- [6] V. Kumar, and N. Michael, "Opportunities and challenges with autonomous micro aerial vehicles," in *International Symposium on Robotics Research*, 2011.
- [7] S. Manning, C. Rash, and P. LeDuc, et al., "The Role of Human Causal Factors in U.S. Army Unmanned Aerial Vehicle Accidents," in *Ft. Rucker, AL: U.S. Army Aeromedical Research Laboratory*, Mar. 2004.
- [8] A. Tvaryanas, W. Thompson, and S. Constable, "U.S. Military Unmanned Aerial Vehicle Mishaps: Assessment of the Role of Human Factors Using Human Factors Analysis and Classification System (HFACS)," in *DC: General Printing Office*, Washington, 2005.
- [9] J. Hing, and P. Oh, "Development of an unmanned aerial vehicle piloting system with integrated motion cueing for training and pilot evaluation," in *Journal of Intelligent and Robotic Systems*, 2009.
- [10] M. Cummings, B. Donmez, and H. Graha, "Assessing the Impact of Haptic Peripheral Displays for UAV Operators," in *Massachusetts Institute of Technology. Dept. of Aeronautics and Astronautics, Humans and Automation Laboratory, Prepared for Charles River Analytics*, 2008.
- [11] T. M. Lam, V. D'Amelio, M. Mulder, and M. M. Van Paassen, "UAV Teleoperation using Haptics with a Degraded Visual Interface," in *IEEE Trans. Systems, Man and Cybernetics*, Oct. 2006.
- [12] H. Xiaolei, R. Mahony, "An intuitive multimodal haptic interface for teleoperation of aerial robots," *Robotics and Automation (ICRA)*, pp. 838-845, May 2014.
- [13] R. Mahony, F. Schill, P. Corke, Y. S. Oh, "A new framework for force feedback



- teleoperation of robotic vehicles based on optical flow," *IEEE International Conference on Robotics and Automation (ICRA)*, pp. 1079-1085, May 2009.
- [14] A. M. Brandt, and M. B. Colton, "Haptic Collision Avoidance for a Remotely Operated Quadrotor UAV in Indoor Environments," in *Systems Man and Cybernetics (SMC), 2010 IEEE International Conference*, Oct. 2010.
- [15] T. M. Lam, H. W. Boschloo, M. Mulder, and M. M. Van Paassen, "Artificial Force Field for Haptic Feedback in UAV Teleoperation," in *IEEE Trans. Systems, Man and Cybernetics, Part A: Systems and Humans*, Nov. 2009.
- [16] A. Franchi, C. Masone, H.H. Bulthoff, P.R. Giordano, "Bilateral teleoperation of multiple UAVs with decentralized bearing-only formation control," *Intelligent Robots and Systems (IROS)*, pp. 2215-2222, September 2011.
- [17] M. Riedel, A. Franchi, H. H. Bülthoff, P. Robuffo Giordano, and H. I. Son, "Experiments on intercontinental haptic control of multiple UAVs," *12th Int. Conf. on Intelligent Autonomous*, June 2012.
- [18] D. Lee, A. Franchi, H. Son, C. Ha, H.H. Bulthoff, P.R. Giordano, "Semiautonomous Haptic Teleoperation Control Architecture of Multiple Unmanned Aerial Vehicles," *IEEE/ASME TRANSACTIONS ON MECHATRONICS*, vol. 18, pp. 1334-1345, August 2013.
- [19] A. Ruesch, A.Y. Mersha, S. Stramigioli, and R. Carloni, "Kinetic scrolling-based position mapping for haptic teleoperation of unmanned aerial vehicles," in *IEEE International Conference on Robotics and Automation*, 2012.
- [20] S. Omari, H. Minh-Duc; G. Ducard, T. Hamel, "Bilateral haptic teleoperation of VTOL UAVs," *Robotics and Automation (ICRA)*, pp. 2393-2399, May 2013.
- [21] S. Weiss, D. Scaramuzza, and R. Siegwart, "Monocular-SLAM-based navigation for autonomous micro helicopters in GPS-denied environments," in *Journal of Field Robotics*, Nov. 2011.
- [22] *NASA Task Load Index (TLX) Instruction Manual, v. 1.0*, Moffett Field. California: Human Performance Research Group, NASA Ames Research Center.
- [23] D. Scott, *Two Finger Solution, Transmitter Handling Tips to Maximize Flying Consistency and Proficiency*, R/C Flight School.
- [24] "Playing Video Games Offers Learning Across Life Span, Say Studies," *American Psychological Association*, 18 August 2008. [Online]. Available: <http://www.apa.org/news/press/releases/2008/08/video-games.aspx>. [Accessed 22 August 2015].



## APPENDIX B

Raw Data of experiment run on the real quadrotor.  
Time taken to finish the trials (in seconds).

VnoF	VF	PnoF	PF	RC						
9.25	8.984	10.297	11.36	10.531	9	10	10.453	11.735	18.609	
10.438	10.734	11.828	16.61	9.969	9.907	14.266	11.813	9.984	10.297	
9.891	8.391	11.438	11.719	10.687	11.828	10.125	14.531	17.828	16.062	
10.812	12.219	12.125	12.547	15.015	8.578	9.953	11.687	13.922	10.532	
13.891	15.016	18.735	13.188	6.953	11.781	11.468	12.422	12.516	9.296	
13.328	11.187	14.172	13.515	11.078	8.563	10.407	13.891	13.89	25.891	
10.296	10.844	12.203	14.64	12.625	12.688	12.609	13.641	15.703	16.813	
10.719	9.406	12.109	11.594	13.484	10.641	8.39	17.438	12.266	13.344	
12.015	9.563	11.593	15.828	17.75						
18.593	11.359	26.828	18.813	27.578						
15.563	12.265	21.266	16.609	19.25						
10.656	10.86	14.266	18.812	25.437						
13.516	12.953	11.984	9.719	9.375						
10.609	11.797	13.219	11.984	13.953						
10.516	13.297	9.422	11.859	11.969						
8.781	11.031	11.297	11.016							
9.703	10.328	10.922	11.047	11.906						
9.172	10.25	10.75	12.547	17						
16.344	9.703	20.407	13.328	15.547						
12.875	9.219	14.922	11.406	15.235						
16.516	10.922	14.188	15.813	23.782						
7.828	11.047	9.141	10.671	9.422						
8.953	10.437	10.344	12.64	9.282						
16.265	9.89	10.406	11.375	15.203						
12.734	9.485	11.219	12.844	13.079						
11.953	13.781	15.937	12.235	12.734						
14.032	9.859	13.219	14.547	11.859						
11.078	10.39		13.329	11.218						
12.171	11.375	13.906	12.672	18.437						
11.078	12.438	16.469	14.344	18.265						
12.906	11.041	14.458	13.208	14.557						
11.093	12.567	16.521	15.588	17.869						
10.63	10.468	14.99	14.953	18.682						
12.109	18.109	14.953	13.969	14.641						
10.015	13.406	16.094	13.781	17.218						
11.157	12.187	12.516	13.015	21.75						
10.125	11.797	12.297	12.063	11.156						

Distance traveled by the UAV (in meters)

VnoF	VF	PnoF	PF	RC					
4.840	3.871	6.477	6.778	5.756	4.822	4.947	5.127	6.389	7.249
5.111	5.489	6.260	6.995	5.446	5.158	4.735	4.313	4.728	6.302
5.462	4.350	5.893	5.523	6.443	3.998	4.458	7.048	5.509	6.715
5.755	5.586	5.389	5.943	5.428	5.383	6.123	6.115	5.088	5.334
6.297	7.972	9.095	5.529	3.623	4.569	4.398	8.799	5.943	4.378
5.395	5.012	5.541	6.463	5.337					
5.388	4.994	5.123	6.864	4.870					
4.929	5.076	5.621	5.357	5.010					
4.697	4.946	5.272	5.220	8.350					
7.477	4.982	9.266	6.535	8.867					
6.053	5.092	7.707	7.372	6.401					
5.747	5.286	5.538	6.640	9.740					
5.290	4.591	6.172	5.137	5.350					
4.384	5.103	4.908	6.414	4.881					
3.841	4.945	4.667	6.624	5.818					
4.694	4.557	5.721	6.346						
5.206	5.277	6.047	7.019	4.477					
4.607	5.239	6.520	4.272	7.137					
7.287	5.117	8.441	5.102	5.353					
5.551	4.926	5.882	5.639	6.803					
7.307	5.418	6.683	7.021	8.572					
4.426	4.585	4.760	5.373	4.619					
4.405	4.611	5.913	4.854	4.406					
6.022	4.987	5.066	5.712	5.510					
4.643	3.886	4.270	5.371	5.055					
5.243	4.700	4.556	4.810	4.847					
6.317	4.152	6.689	5.443	5.360					
5.388	5.247		5.934	4.904					
5.415	5.455	5.508	5.538	5.742					
5.628	5.740	6.082	6.416	8.364					
5.401	4.246	5.171	5.208	5.087					
5.676	5.280	7.721	6.616	6.516					
4.650	4.993	7.321	5.513	5.476					
6.370	5.442	10.125	6.181	5.893					
5.228	5.494	6.609	8.068	5.523					
5.430	4.904	6.430	5.599	8.133					
4.937	4.943	4.433	4.957	5.130					
4.273	4.178	4.375	4.405	9.724					
4.420	4.922	5.048	4.936	4.763					
5.696	6.510	4.949	6.718	8.476					

Overshooting from the landing destination (in meters)

VnoF	VF	PnoF	PF	RC					
1.3429	0.2868	0.4536	0.6078	0.5844	0.6426	0.1866	1.7264	0.2618	0.3079
0.5691	0.1539	0.8308	0.5294	0.6230	0.1874	0.6057	0.7227	0.2230	0.0486
0.1692	0.2058	0.4978	0.8105	0.2792	0.1922	0.4771	0.5756	0.2453	0.7761
0.2215	0.1286	0.2923	0.1904	0.0460	0.1360	0.2011	0.4347	0.1724	0.8431
0.1873	0.6799	0.6208	0.2123	0.1574					
0.2329	0.3875	0.5055	0.3510	0.2585					
0.0797	0.0263	0.2030	0.6107	0.2309					
0.1238	0.5317	0.2446	0.2583	0.4200					
0.1436	0.3240	0.4623	0.7758	0.8058					
0.2262	0.1817	0.7363	0.4017	0.2523					
0.2715	0.6152	0.2788	0.2662	0.2035					
0.1079	0.5332	0.3058	0.1554	0.6029					
0.4969	0.3964	0.5414	0.0385	0.3126					
0.2663	0.3259	0.7005	0.4362	0.3876					
0.6735	0.2549	0.3105	0.8344	0.4618					
1.0124	0.4666	0.6859	0.7614						
0.6587	0.2192	1.0094	1.0141	0.4245					
0.4965	0.1771	0.6472	0.6227	0.8934					
0.5758	0.2412	0.5408	1.1241	0.3597					
0.2636	0.1495	0.4545	0.5507	0.2959					
0.3323	0.0975	0.7943	0.2359	0.1789					
0.1665	0.5620	0.6500	0.2019	0.1425					
0.3344	0.0429	0.7564	0.5415	0.4062					
0.5598	0.5195	0.9819	0.3509	0.1159					
0.1762	0.1297	0.4477	0.4854	0.2768					
0.5520	0.1539	0.1429	0.1504	0.4953					
0.2795	0.2362	0.3557	0.2295	0.2141					
0.1615	0.3424		1.0452	0.2373					
0.2688	0.2539	0.5533	0.1779	0.7621					
0.8725	0.7176	0.4265	0.2923	0.7646					
0.3359	0.1733	0.3154	0.4884	0.3288					
0.3309	0.4591	1.1448	0.3622	0.9558					
0.1719	0.4280	0.5777	0.4136	0.5559					
0.5876	0.3636	1.7413	0.2473	0.3945					
0.1323	0.5869	1.1015	0.5971	0.9359					
0.2729	0.4269	0.5915	0.2423	1.5368					
0.3549	0.2009	0.9769	0.3375	0.2987					
0.0476	0.1077	0.3073	0.0564	0.3387					
0.4148	0.4221	0.1891	0.4578	0.4266					
1.0955	0.1330	1.4495	0.1499	0.2596					
0.4216	0.3985	0.7629	0.4011	0.4575					

